

Polylactide-Layered Silicate Nanocomposite: A Novel Biodegradable Material

Suprakas Sinha Ray,[†] Kazunobu Yamada,[‡] Masami Okamoto,^{*,†} and Kazue Ueda[‡]

Advanced Polymeric Materials Engineering, Graduate School of Engineering, Toyota Technological Institute, Hisakata 2-12-1, Tempaku, Nagoya 468 8511, Japan, and Unitika Ltd. Kozakura 23, Uji, Kyoto 611-0021, Japan

Received July 16, 2002

ABSTRACT

This letter describes the preparation, characterization, material properties, and biodegradability of polylactide (PLA)-layered silicate nanocomposite. Montmorillonite modified with trimethyl octadecylammonium cation was used as an organically modified layered silicate (OMLS) for the nanocomposite preparation. WAXD and TEM analyses respectively confirmed that silicate layers of the montmorillonite were intercalated and nicely distributed in the PLA-matrix. The material properties of neat PLA improved remarkably after nanocomposite preparation. The biodegradability of the neat PLA and corresponding nanocomposite was studied under compost, and the rate of biodegradation of neat PLA increased significantly after nanocomposite preparation.

Today, tremendous amounts and varieties of plastics, notably polyolefins, polystyrene, and poly(vinyl chloride), are produced mostly from fossil fuels, then consumed and discarded into the environment, ending up as spontaneously undegradable wastes. Disposal of these materials by incineration always produces CO₂ and contributes to global pollution, and some but not all of these plastics even release toxic gases on incineration. For these reasons, there is an urgent need for the development of “green polymeric materials” that do not involve the use of toxic or noxious components in their manufacture, and that could compost to naturally occurring degradation products. Accordingly, polylactide (PLA) is of increasing interest because it is made from renewable sources and its properties are benign to the environment.¹

In our recent papers,^{2,3} we have reported the successful preparation of PLA-organically modified layered silicate (OMLS) nanocomposites by melt extrusion of PLA and montmorillonite (mmt) modified with octadecylammonium cation (C₁₈-mmt). WAXD analyses and TEM observations respectively established that silicate layers of the clay were intercalated, stacked, and randomly distributed in the matrix. The intercalated PLA/C₁₈-mmt nanocomposites exhibited remarkable improvement of mechanical properties in both solid and melt states as compared to that of neat PLA.

The main objective of this letter is to investigate the concurrent improvement of mechanical properties, various practical material properties, and biodegradability of PLA after nanocomposite preparation with trimethyl octadecylammonium-modified montmorillonite (C³C₁₈-mmt), and this is the first report in which we will describe the biodegradability of neat PLA and PLA/C³C₁₈-mmt nanocomposite in compost.

PLA with D content of 1.1–1.7% was supplied by Unitika Co. Ltd., Japan, and was dried under vacuum at 60 °C and kept under dry nitrogen gas prior to use. The C³C₁₈-mmt used in this study was supplied by Hojun Yoko Co. Ltd., Japan, and was synthesized by replacing Na⁺ in mmt (thickness ~1 nm and length ~100 nm) of a cation exchange capacity (CEC) of 90 mequiv/100 g with trimethyl octadecylammonium cation by ion exchange reaction.

The nanocomposite was prepared by melt extrusion. C³C₁₈-mmt (powder form) and PLA (pellet form) were first dry-mixed by shaking them in a bag. The mixture was then melt extruded using a twin-screw extruder (PCM-30, Ikegai machinery Co.) operated at 210 °C⁴ (screw speed = 100 rpm, feed rate = 120 g/min) to yield strand of the nanocomposite. Henceforth, the product nanocomposite was abbreviated as PLACN. The PLACN prepared with 4 wt % of C³C₁₈-mmt was abbreviated as PLACN4. The extruded strand was then pelletized and dried under vacuum at 60 °C for 48 h to remove any water. The dried PLACN4 pellets were then converted into sheets with a thickness of 0.7 to 2 mm by pressing with ~1.5 MPa at 190 °C for 3 min.

* Corresponding author. Tel.: +81-52-809-1861; fax: +81-52-809-1864; e-mail: okamoto@toyota-ti.ac.jp.

[†] Toyota Technological Institute.

[‡] Unitika Ltd.

The number-average (M_n) and weight-average (M_w) molecular weights of the PLA-matrix were determined from GPC (LC-VP, Shimadzu Co.), which was based on the calibration using polystyrene standards and tetrahydrofuran (THF) as a carrier solvent at 40°C with the flow rate of 0.5 mL/min. The GPC results show very slight degradation of PLA matrix after nanocomposite preparation ($M_w = 177$ K of PLA becomes 165 K for PLACN4) with C³C₁₈-mmt.

WAXD analyses were performed for the C³C₁₈-mmt powder, neat PLA, and PLACN4 using a MXlabo diffractometer (MAC Science Co.), which has a X-ray generator of 3 kW, a graphite monochromator, Cu K α radiation (wavelength, $\lambda = 0.154$ nm), and was operated at 40 kV/20 mA. The samples (PLA and PLACN4) were isothermally crystallized at 110 °C for 1.5 h) were scanned in fixed time (FT) mode with counting time of 2 s under the diffraction angle 2 Θ in the range of 1° to 70°.

To clarify the nanoscale structure of the intercalated PLACN4, a TEM (H-7100, Hitachi Co.) was also used and operated at an accelerating voltage of 100 kV. The ultrathin sections (the edge of the sample sheets) with a thickness of 100 nm were microtomed at -80 °C using a Reichert Ultra cut cryoultramicrotome without staining.

The dynamic mechanical properties of neat PLA and PLACN4 were measured by using a Rheometrics dynamic analyzer (RDAII) in the tension-torsion mode. The details were described elsewhere.²

The dried neat PLA and PLACN4 pellets were injection molded to test specimens using an injection machine (IS-80G, Toshiba Machinery Co.) operated at 190 °C with the mold temperature of 30 °C. Flexural modulus and other mechanical properties of the injection-molded specimens (thickness = 3.2 mm), annealed at 120 °C for 30 min, were measured according to ASTM D-790 method (model 2020, Intesco Co.) with strain rate of 2 mm/min at room temperature. We also conducted heat distortion tests (injection molded samples, HDT tester, Toyoseiki Co.) according to ASTM D-648 method with heating rate of 2 °C/min.

The oxygen gas transmission rate of neat PLA and PLACN4 was measured at 20 °C and 90% relative humidity by the ASTM D-1434 differential pressure method (GTR-30XAU, Yanaco Co.). Test samples were prepared by compression molding (thickness = ~300 μ m), and melt quenched amorphous samples were used for this measurement.

Biodegradability of the neat PLA and PLACN4 was studied by our own compost instrument (Compost SB-FM) at 58 ± 2 °C. The compost used was food waste compost, and was supplied by Japan Steel Works, Ltd. The test specimens were prepared by compression molding with a thickness of 1 mm. The shape of the original test samples (crystallized at 110 °C for 1.5 h) was 3 × 10 × 0.1 cm³.

The WAXD patterns of C³C₁₈-mmt powder, the neat PLA, and PLACN4 in the range of 2 Θ = 1–10° are presented in Figure 1a. The pattern of the neat PLA is displayed as a baseline to compare the existence of diffraction peaks coming from C³C₁₈-mmt dispersed in the matrix. The gallery spacing (d_{001}) of C³C₁₈-mmt powder is 1.93 nm (2 Θ ≈ 4.56°). This

Table 1: Comparison of Material Properties between Neat PLA and PLACN4

material properties	neat PLA	PLACN4
storage modulus/GPa at 25 °C	1.63	2.32
flexural modulus/GPa at 25 °C	4.8	5.5
flexural strength/MPa at 25 °C	86	134
distortion at break/%	1.9	3.1
HDT/°C	76.2	94
O ₂ gas permeability coefficient (mL.mm.m ⁻² .day ⁻¹ .MPa ⁻¹)	200	177

value increases to about 3.05 nm in the case of PLACN4. These results clearly indicate that some of the PLA chains are intercalated between the silicate layers.

Figure 1b shows the typical result of a TEM bright field image of PLACN4 in which dark entities are the cross section of intercalated silicate layers. In the TEM image, we observed stacked and intercalated silicate layers with large anisotropy, which have an original thickness of ~1 nm and average length of ~100 nm. The average size of the stacked, intercalated, and flocculated silicate layers appears to reach about 200 nm in length, and which are nicely distributed in the PLA matrix. However, we cannot estimate the thickness precisely from the TEM image.

In Table 1 we report the storage modulus, flexural properties and heat distortion temperature of neat PLA and PLACN4 measured at 25 °C. There is a significant increase of storage modulus, flexural properties, and HDT for PLACN4 compared to that of neat PLA.

The nanoclays are believed to increase the barrier properties by creating a maze or “tortuous path” that retard the progress of gas molecules through the matrix resin.⁵ The O₂ gas permeability coefficients for the neat PLA and PLACN4 are presented in Table 1. According to the Nelsen model,⁶ when plates of length ($\approx L_{\text{clay}}$) and width ($\approx D_{\text{clay}}$) of the clay, which are dispersed parallel in polymer matrix, then the tortuosity factor (τ) can be expressed as

$$\tau = 1 + (L_{\text{clay}}/2D_{\text{clay}})\phi_{\text{clay}}$$

where ϕ_{clay} is the volume fraction of dispersed clay particles. Therefore, the relative permeability coefficient ($P_{\text{PLACN4}}/P_{\text{PLA}}$) is given by

$$P_{\text{PLACN4}}/P_{\text{PLA}} = \tau^{-1} = 1/[1 + (L_{\text{clay}}/2D_{\text{clay}})\phi_{\text{clay}}]$$

where P_{PLACN4} and P_{PLA} are the O₂ gas permeability coefficients of PLACN4 and neat PLA, respectively. In the case of PLACN4, the value of $L_{\text{clay}} = \sim 200$ nm (from TEM), and the value of $D_{\text{clay}} = 12.25$ nm (as calculated by using Scherrer equation).⁷ Therefore, the calculated value of $P_{\text{PLACN4}}/P_{\text{PLA}}$ is equal to 0.896. The experimental value of 0.885 is well matched with the above model but slightly lower than the calculated one. Presumably, the planer orientation of the dispersed clay particles in the compression-molding sheet is not sufficient.

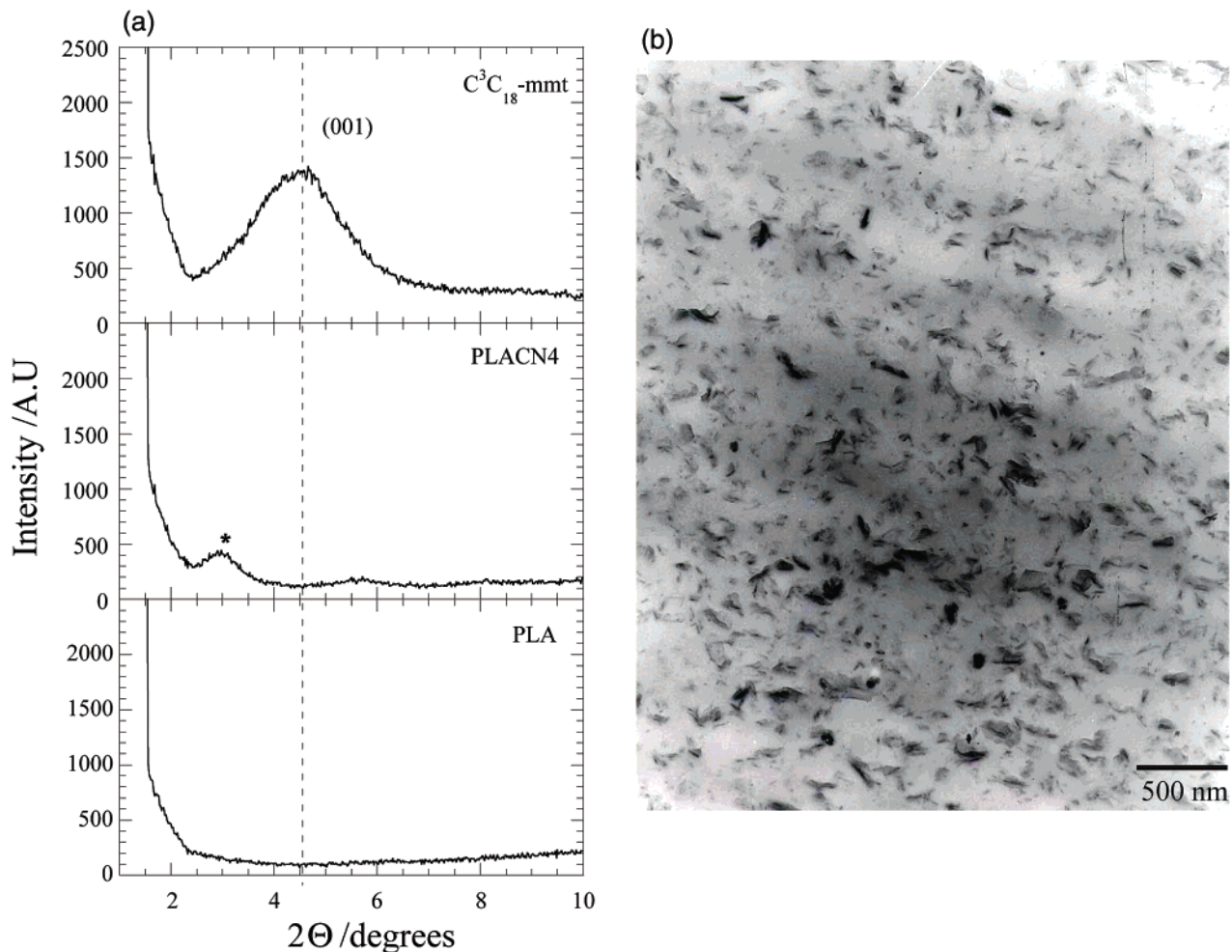


Figure 1. (a) WAXD patterns for $\text{C}^3\text{C}_{18}\text{-mmt}$ powder, neat PLA, and PLACN4. The dashed line indicates the location of the silicate (001) plane reflection of $\text{C}^3\text{C}_{18}\text{-mmt}$. The asterisk indicates the (001) peak for PLACN4. (b) TEM bright field image of PLACN4. The dark entities are the cross section of the stacked and intercalated silicate layers and bright areas are the matrix.

The most interesting and exciting aspect of this research is the significant improvement of biodegradability of neat PLA after nanocomposite preparation. Very recently, Lee et al.⁸ reported the biodegradation of aliphatic polyester based nanocomposites under compost. They assumed that the retardation of biodegradation was due to the improvement of the barrier properties of the aliphatic polyester after nanocomposite preparation with clay. However, there is no data about permeability.

Figure 2a shows the real picture of the recovered samples of PLA and PLACN4 from the compost with time. The decreased M_w and residual weight percentage of the initial test samples with time are also reported in Figure 2b. Obviously, the biodegradability of neat PLA is significantly enhanced after nanocomposite preparation with $\text{C}^3\text{C}_{18}\text{-mmt}$. Within one month, both extent of M_w and extent of weight loss are almost same level for both PLA and PLACN4. However, after one month, a sharp change occurs in weight loss of PLACN4, and within two months, it is completely degraded in compost. The degradation of PLA in compost is a complex process involving four main phenomena, namely, water absorption, ester cleavage and formation of oligomer fragments, solubilization of oligomer fragments,

and finally diffusion of soluble oligomers by bacteria.⁹ Therefore, the factor that increases the hydrolysis tendency of PLA ultimately controls the degradation of PLA.

We expect that the presence of terminal hydroxylated edge groups of the silicate layers may be one of the responsible factors for this behavior. In the case of PLACN4, the stacked (~ 4 layers) and intercalated silicate layers are homogeneously dispersed in the PLA matrix (from TEM image), and these hydroxy groups start heterogeneous hydrolysis of the PLA matrix after absorbing water from compost. This process takes some time to start. For this reason, the weight loss and degree of hydrolysis of PLA and PLACN4 is almost the same up to one month (Figure 2b). However, after one month there is a sharp weight loss in case of PLACN4 compared to that of PLA. This means that one month is a critical value to start heterogeneous hydrolysis, and due to this type of hydrolysis the matrix becomes very small fragments and disappears with compost. This assumption was confirmed by conducting the same type of experiment with PLACN prepared using a dimethyl dioctadecylammonium salt-modified synthetic mica that has no terminal hydroxylated edge group, and a degradation tendency almost the same as that of neat PLA.

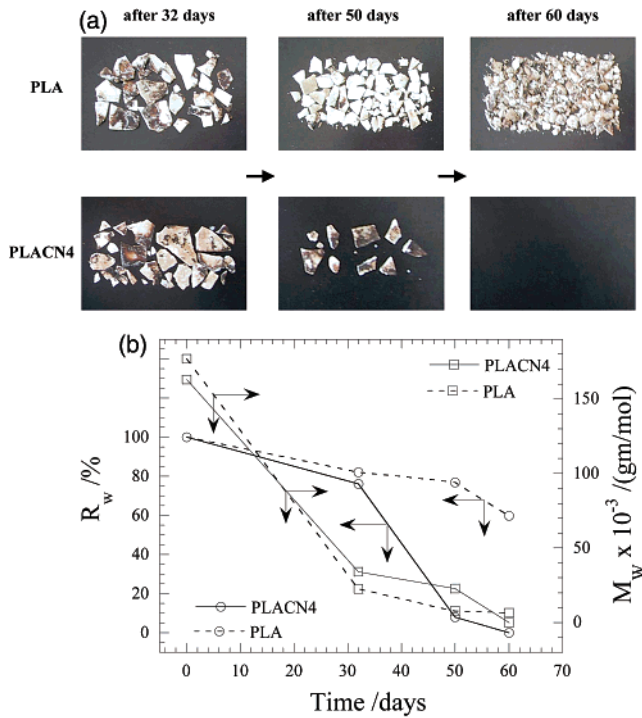


Figure 2. (a) The real picture of biodegradability of neat PLA and PLACN4 recovered from compost. The initial shape of the crystallized samples was $3 \times 10 \times 0.1 \text{ cm}^3$. (b) Time dependence of residual weight, R_w (%) and change of matrix M_w of neat PLA and PLACN4.

In conclusion, we describe a novel nanocomposite approach for biodegradable polylactide that results in a significant improvement in practical material properties with a simultaneous improvement in biodegradability.

Acknowledgment. Thanks are due to the Japan Society for the Promotion of Science (JSPS) for the award of JSPS Postdoctoral Fellowship (ID No. P02152) and a research grant to S.S.R.

References

- Grijpma, D. W.; Pennings, A. J. *Macromol. Chem. Phys.* **1994**, *195*, 1649. Perego, G.; Cella, G. D.; Bastioli, C. *J. Appl. Polym. Sci.* **1996**, *59*, 37. Sinclair, R. G. *J. Macromol. Sci.-Pure Appl. Chem.* **1996**, *A33*, 585. Tsuji, H.; Ikada, Y. *J. Appl. Polym. Sci.* **1998**, *67*, 405. Martin, O.; Averous, L. *Polymer* **2001**, *42*, 6209.
- Sinha Ray, S.; Maiti, P.; Okamoto, M.; Yamada, K.; Ueda, K. *Macromolecules* **2002**, *35*, 3104.
- Sinha Ray, S.; Okamoto, K.; Yamada, K.; Okamoto, M. *Nano Lett.* **2002**, *2*, 423.
- We have checked the degradation of intercalated trimethyl octadecylammonium salt by using thermogravimetric (TG) analysis. Up to 210°C , there is no degradation of intercalated organic salt. After 272°C there is a 5% degradation.
- Yano, K.; Usuki, A.; Okada, A.; Kurauchi, T.; Kamigaito, O. *J. Polym. Sci. A: Polym. Chem.* **1993**, *31*, 2493. Kojima, Y.; Usuki, A.; Kawasumi, M.; Fukushima, Y.; Okada, A.; Kurauchi, T.; Kamigaito, O. *J. Mater. Res.* **1993**, *8*, 1179. Messersmith, P. B.; Giannelis, E. P. *J. Polym. Sci. A: Polym. Chem.* **1995**, *33*, 1047. Xu, R.; Manias, E.; Snyder, A. J.; Runt, J. *Macromolecules* **2001**, *34*, 337.
- Nielsen, L. *J. Macromol. Sci. Chem.* **1967**, *A1*(5), 929.
- $D = (k\lambda)/(\beta \cos \Theta)$, where k is a constant and is equal to 0.9; λ is the wavelength of X-ray (here $\lambda = 0.154 \text{ nm}$); β is the half width of the WAXD peak and measured from the half of the intensity of the peak; Θ corresponds to the WAXD peak. Drits, V. A.; Tchoubar, C. *X-ray Diffraction by Disordered Lamellar Structures*; Springer-Verlag: New York, 1990; 99 21–22. Cullity, B. D. *Principles of X-ray Diffraction*; Addison-Wesley: Reading, MA, 1978.
- Lee, S. R.; Park, H. M.; Lim, H.; Kang, T.; Li, X.; Cho, W. J.; Ha, C. S. *Polymer* **2002**, *43*, 2495.
- Liu, J. W.; Zhao, Q.; Wan, C. X. *Space Medicine Medical Eng. (Chinese)* **2001**, *14*, 308. Lunt, J. *Polym. Degrad. Stab.* **1998**, *59*, 145.

NL0202152